Symmetry-breaking effects upon bipartite and multipartite entanglement in the *XY* model

Thiago R. de Oliveira,* Gustavo Rigolin,† Marcos C. de Oliveira,‡ and E. Miranda§
Instituto de Física Gleb Wataghin, Universidade Estadual de Campinas, Caixa Postal 6165, CEP 13083-970, Campinas, São Paulo, Brazil

(Received 7 September 2007; published 14 March 2008)

We analyze the bipartite and multipartite entanglement for the ground state of the one-dimensional *XY* model in a transverse magnetic field in the thermodynamical limit. We explicitly take into account the spontaneous symmetry breaking in order to explore the relation between entanglement and quantum phase transitions. As a result we show that while both bipartite and multipartite entanglement can be enhanced by spontaneous symmetry breaking deep into the ferromagnetic phase, only the latter is affected by it in the vicinity of the critical point. This result adds to the evidence that multipartite, and not bipartite, entanglement is the fundamental indicator of long-range correlations in quantum phase transitions.

DOI: 10.1103/PhysRevA.77.032325 PACS number(s): 03.67.Mn, 03.65.Ud, 05.30.−d

I. INTRODUCTION

One of the most remarkable features of many phase transitions is the occurrence of spontaneous symmetry breaking, in which the symmetry of the Hamiltonian is not realized in the system state. When this occurs a macroscopic observable (the order parameter) emerges, which is required for a unique specification of the microscopic state [1]. Those quantum phase transitions (QPT) occur at zero temperature, and are triggered by the variation of a parameter of the system's Hamiltonian [2]. The system's eigenenergies then show nonanalytical behavior which embodies the order of the phase transition. These nonanalyticities in turn are reflected in several macroscopic observables.

Lately there has been an increasing interest in describing QPTs, not by means of the nonanalyticities of the spectrum or of the physical observables, but rather by the amount of entanglement (bipartite or multipartite) present in each of the system's phases. This is motivated in particular by a general expectation that entanglement can be given as important a status as the energy: both quantities can be seen as resources useful for the accomplishment of interesting physical tasks [3]. Moreover, long-range correlations often found in strongly correlated many-body systems at zero temperature have a purely quantum origin and are expected to be inextricable from entanglement [4,5]. Several authors have studied the role of entanglement in QPTs by considering either bipartite or multipartite entanglement measures (e.g., see Refs. [6–36]), both calculated for spin-1/2 lattice models such as the Ising and *XY* model in a transverse magnetic field [37–40]. Invariably though many of these developments do not take into account the spontaneous symmetry breaking accompanying the QPT, employing instead symmetric states in calculations in the ordered phase (for an exception see Refs. [52,53] and the note at the end of the manuscript). This procedure, although common and even correct for finite systems, is unrealistic in the study of QPTs since it is well known that symmetric states (Schrödinger cats) are never realized in the thermodynamic limit due to superselection rules [1].

Recently, we have developed a program on the investigation of multipartite entanglement properties in QPTs by proposing a generalized global entanglement (GGE) measure [41,42]. As the name suggests this is a generalization of the Meyer and Wallach global entanglement [43] [here dubbed $G(1)$] to account for all the possible bipartitions of the system state. In addition to being able to detect any kind of entanglement present in the system [42], this measure is also able to signal the location and the type (order) of QPTs [44]. Our results developed for the infinite one-dimensional (1D) Ising and *XY* chains indicate that multipartite entanglement is maximal at the critical point, playing a major role in the QPT process, in contrast to bipartite entanglement [6,7].

To correctly consider the spontaneous symmetry breaking due to quantum fluctuations is an essential element for the success of such an entanglement measure. However, this point is particularly unclear in the recent literature on entanglement in QPTs. Many authors are not specific in their choices and have erroneously applied a symmetric state in their investigations. In this article we extend the entanglement analysis for the *XY* model taking into account the role played by spontaneous symmetry breaking in both bipartite (pairwise) and multipartite entanglement. As we argue in the body of the paper, symmetry breaking favors multipartite entanglement. While bipartite measures (concurrence and negativity) are the same irrespective of the state one is employing, multipartite entanglement is not. We show that both $G(1)$ as well as $G(2,n)$, an auxiliary function defining one class of GGE, exhibit completely different behaviors depending on whether the state is symmetric or not. We also review some of the results on bipartite and multipartite entanglement in a clearer and more detailed fashion. We expect with this work to settle some issues concerning the relation between entanglement and quantum phase transitions, at least in the context of the one-dimensional *XY* model. This paper is structured as follows. In Sec. II we review the essential results in the literature regarding bipartite and multipartite entanglement present in the 1D Ising and *XY* models. In Sec.

*tro@ifi.unicamp.br
†rigolin@ifi.unicamp.br
‡marcos@ifi.unicamp.br
§emiranda@ifi.unicamp.br

III we discuss the *XY* model in detail and show how the reduced two-spin state is calculated. In Sec. IV we analyze bipartite entanglement measures (concurrence and negativity) by comparing the results obtained for the symmetric state with the ones obtained for the broken-symmetry one. In Sec. V we analyze the multipartite entanglement as given by $G(1)$ and $G(2,1)$ for the two choices of ground states (symmetric or broken symmetry). Finally, in Sec. VI a discussion ends the paper.

II. ENTANGLEMENT AND QPT IN 1D ISING AND *XY* SPIN CHAINS

In this section we outline some of the most relevant findings [45] associated with entanglement in the 1D Ising and *XY* models. The first approach we mention, concerning pairwise entanglement (concurrence) between two spins in the chain, was considered in Refs. [6,7]. It was demonstrated that the concurrence between nearest neighbors of the *XY* model is maximal not at the critical point but in its vicinity. Furthermore, the pairwise entanglement between neighbors more than three sites apart vanishes in the quantum Ising chain. The authors of Ref. [7] also showed that the derivative of the nearest-neighbor concurrence is able to signal the QPT as it diverges at the critical point and exhibits finite-size scaling. Thus, it became clear that the ability to signal a QPT could be a general property of good entanglement measures.

The first work to establish a formal relation between a QPT and bipartite entanglement measures was Ref. [8]. The authors have demonstrated that, under a set of reasonable assumptions, a discontinuity in a bipartite entanglement measure (concurrence [9] and negativity [10]) is a necessary and sufficient indicator of a first order quantum phase transition (1QPT), which is generically characterized by a discontinuity in the first derivative of the ground-state energy. Furthermore, they have shown that a discontinuity or a divergence in the first derivative of the same measure (assuming it is continuous) is a necessary and sufficient indicator of a second order QPT (2QPT), which is generically characterized by a discontinuity or a divergence of the second derivative of the ground-state energy. Subsequently, it was pointed out [11] that this result was more general and would apply to any entanglement measure dependent on the reduced density operator of two spins. Finally, it was demonstrated in Ref. [12], using the density functional theory formalism, that any entanglement measure can be expressed as a unique functional of the set of first derivatives of the ground-state energy. For most of the cases, however, the explicit expression of the functional is not known. This result showed that any entanglement measure can, in principle, signal a QPT, since it inherits the nonanalytical behavior of the derivative of the energy. Of course, depending on the definition of the entanglement measure used, "accidental" cancellations of such divergences or discontinuities may occur (see Refs. [13,14]). Another approach to understand pairwise entanglement in QPTs based on the study of the crossing of energy levels has also been proposed [15]. For the case of a system of indistinguishable particles it was proved that, given some provisos, the entanglement between one part (A) and the rest (B) is able to signal a QPT [16]. However, in this case parts A and B correspond to modes not particles, in contrast to the former mentioned works. We should also note that pairwise entanglement in small chains (two, three, and four spins) for the *XY* model was previously studied in Ref. [17].

The second kind of approach worth mentioning focuses on multipartite entanglement (ME). In Refs. [18,19] the entropy of entanglement between one part of the chain (a block of L spins) and the rest is employed for this purpose. There the entanglement entropy is defined through the von Neumann entropy of one of the reduced parts, a valid approach whenever the global state is pure. It was shown for some spin-1/2 models that at the critical point (CP) the entanglement entropy increases logarithmically with L, whereas it saturates for large L away from the CP, a result which had been known from conformal field theory [20,21]. For the one-dimensional *XY* model the block entanglement was extensively and carefully studied in Ref. [22]. Another approach for ME investigation is considered in Ref. [23] through the study of the maximal possible overlap between the state studied and all possible separable states; the larger this overlap is, the less entangled the state. The *XY* model was analyzed in that way and it was shown that the ME is maximal around the CP and its derivatives diverge as the CP is approached. It was also shown that the ME is zero at the second critical point (2CP) where the state is known to be separable [24] (see the discussion in Sec. IV). Tripartite entanglement, given in terms of the residual tangle [25], was also analyzed for an Ising chain of three spins in a transverse field in Ref. [26]. In this last work it was shown that the residual tangle is not maximal around the expected CP, which really exists only in the thermodynamic limit. With the purpose of studying ME, a new measure was defined and analyzed for spin chains in Ref. [27]. It was named localizable entanglement and defined as the maximal amount of entanglement that can be localized in two particles, on average, by doing local measurements on the rest of the particles. The localizable entanglement was shown to be maximal at the "critical" point for a finite Ising chain of 14 spins. This, together with the results for the block entanglement, were the first evidences that multipartite entanglement could be important in the context of quantum phase transitions. It was also demonstrated that connected correlation functions are a lower bound for localizable entanglement, a remarkable result enabling the system to have a finite correlation length but infinite entanglement length (see Ref. [28] for an example of such behavior). We should remark, however, that it has been argued that localizable entanglement may not be an entanglement monotone [29].

With the hope that the tools of quantum information and computation could help to better understand quantum phase transitions Zannardi and co-workers [30] have proposed and (in their own words) "showed that quantum fidelity—the overlap modulus—of two finite-size ground states corresponding to neighboring control parameters is a good indicator of quantum phase transitions. Indeed, the fidelity typically drops abruptly at the critical points, as a consequence of the dramatic state transformation involved in a transition." For the sake of completeness we should also mention studies of the temporal evolution of the entanglement in the *XY*

chain [31] as well as other attempts to show that multipartite entanglement is important and enhanced in quantum phase transitions, as can be found in Refs. [24,32–35].

We note that none of the employed entanglement measures in the above studies are maximal at the CP, with the exception of the single site entropy of the Ising model [6] in the thermodynamic limit and the localizable entanglement [27] of an Ising chain of a few spins. We should also mention that in Ref. [36] the authors have studied the loss of entanglement along the renormalization group flow of an *XY* chain. For this purpose they obtained the entanglement between 100 spins and the rest of the chain, as a function of the transverse magnetic field and the anisotropy, showing that it was indeed maximal at the critical point.

At this point we should mention another interesting feature observed in Refs. [6,7], independently. They showed that bipartite entanglement vanishes when the distance between the two spins is greater than one lattice site. This is quite surprising since long-range quantum correlations are expected to be present at the CP. It was then conjectured that bipartite entanglement at the CP would decrease in order for the ME to increase, due to entanglement sharing [6]. In other words, ME only appears at the expense of pairwise entanglement and at the CP we should expect a genuine multipartite entangled state.

In Refs. [41,42] three of us used the fact that for the quantum Ising chain the entanglement between one spin and the rest of the chain (given by the averaged linear entropy [46]) is equal to the global entanglement (GE) $G(1)$, a proposed ME measure introduced by Meyer and Wallach in 2002 [43], in order to show that $G(1)$ is maximal at the critical point. Inspired by the GE, we have also proposed the GGE $E_G^{(n)}$, where the averages are taken over the linear entropy of two, three, and more spins (or subsystems). A similar approach was independently presented in Ref. [47]. In that construction, we allow the spins to be noncontiguous along the chain and not just in a continuous block as already considered in Refs. [18,19]. For example, $E_G^{(2)}$ is the entanglement between two spins and the rest of the chain averaged over all possible distances between the spins. In this context, another quantity that is also interesting is the average entanglement between two spins n sites apart and the rest of the chain (without averaging over n): $G(2,n)$. In Refs. [41,42] we then analyzed the entanglement between two spins n sites apart $[G(2,n)]$ and the rest of the chain showing that it is maximal at the critical point and increases with n, saturating at the value 0.675 in the limit of large n. This result was one of the first indications that multipartite entanglement is maximal or enhanced and more distributed at the critical point, adding strength to the conjecture of Osborne and Nielsen [6]. It also suggested that ME is the key ingredient for the appearance of the long-range correlations that develop at the critical point. In Ref. [42] we have pursued the discussion of Ref. [41] further, exploring the advantageous features of the generalized global entanglement for an operational multipartite entanglement classification and quantification, in comparison to the other available measures for both finite and infinite collections of two-level systems.

In a more recent work [44], we extended the above results to the one-dimensional *XY* model showing that $G(1)$ and $G(2,n)$ are maximal at the critical point. In a more general context we also showed explicitly that $G(2,n)$ is able to signal QPTs, something already expected from the results of Refs. [11,12]. Finally, and more striking, we demonstrated that for collections of two-level systems with symmetry-breaking second-order quantum phase transitions, $G(2,n)$ increases exponentially with n away from the critical point. This increase is governed by a characteristic length, named the entanglement length ξ_E, which is half the correlation length $\xi_E=\xi_C/2$. Furthermore, at the critical point, $G(2,n)$ increases as a power law, implying an infinite entanglement length. In fact, ξ_E inherits the full critical behavior of ξ_C, with the same critical exponent. All these results indicate again that multipartite entanglement plays a major role at quantum phase transitions, as argued in the previous paragraph. How important is the spontaneous symmetry breaking for this conclusion? In the next sections we develop this question for the 1D *XY* spin chain.

III. *XY* MODEL AND THE TWO SPIN REDUCED DENSITY MATRIX

The one-dimensional *XY* model in a transverse field is governed by the following Hamiltonian:

$$H=-\sum_{i=1}^{N}\frac{J}{2}[(1+\gamma)\sigma_i^x\sigma_{i+1}^x+(1-\gamma)\sigma_i^y\sigma_{i+1}^y]+h\sum_{i=1}^{N}\sigma_i^z, \tag{3.1}$$

where σ_i^α, $\alpha=x,y,z$, are the usual Pauli matrices. The model reduces to the quantum Ising model for $\gamma=1$ and approaches the *XX* model [39] as $\gamma\to 0$. The *XX* model belongs to a different universality class and we will therefore focus only on the parameter range $0<\gamma\leq 1$.

The Hamiltonian (3.1) is symmetric under a global π rotation about the z axis ($\sigma^{x(y)}\to-\sigma^{x(y)}$), which usually implies a zero value for the magnetization in the x or y direction ($\langle\sigma^{x(y)}\rangle=0$). However, as the magnetic field h is decreased (or J increased) this symmetry is spontaneously broken in the ground state (in the thermodynamic limit) at $\lambda=J/h=\lambda_1\equiv 1$, the first critical point (1CP). More specifically, the ground state is doubly degenerate with a finite magnetization ($\langle\sigma^x\rangle=\pm M$) in the x direction characterizing a ferromagnetic phase. It is also possible to define a symmetric ground state ($\langle\sigma^x\rangle=0$) using a superposition of the two degenerate ones. Nonetheless, symmetric macroscopic states are just a theoretical construction with no physical existence, since spontaneous symmetry-breaking mechanisms (superselection) rapidly destroy such coherent superpositions (Schrödinger cats) in the thermodynamic limit [48]. These unphysical states are called here symmetric states in contrast with the realistic broken-symmetry ones ($\langle\sigma^x\rangle=\pm M$). Note that in the paramagnetic phase ($\lambda\leq 1$) there exists no such distinction.

By further decreasing the magnetic field a second phase transition occurs at $\lambda=\lambda_2(\gamma)\equiv 1/\sqrt{1-\gamma^2}$, the second critical point (2CP). For magnetic fields smaller than this critical value, the correlation functions do not tend to their limiting value monotonically but in an oscillatory fashion [39]. The

Ising limit $\gamma=1$ exhibits only the first critical point.

As we will show in the following two Sections, for the calculation of the bipartite and multipartite [$G(1)$ and $G(2,n)$] entanglement all we need is the reduced density matrix of two spins, a 4×4 matrix that can be expanded in tensor products of Pauli matrices and the identity σ^0:

$$\rho_{i,j}=\frac{1}{4}\sum_{\alpha,\beta}p_{i,j}^{\alpha,\beta}\sigma_i^\alpha\otimes\sigma_j^\beta, \tag{3.2}$$

where

$$p_{i,j}^{\alpha,\beta}=\mathrm{Tr}[\sigma_i^\alpha\otimes\sigma_j^\beta\rho_{i,j}]=\langle\sigma_i^\alpha\otimes\sigma_j^\beta\rangle. \tag{3.3}$$

The reduced density matrix $\rho_{i,j}$ is obtained by tracing out all spins other than i and j.

Remembering that $\rho_{i,j}$ is Hermitian with a unitary trace we are left with nine independent matrix elements for $\rho_{i,j}$, which are functions of the nine possible one-and two-point correlation functions ($p_{i,j}^{\alpha,\beta}=p_{i,j}^{\beta,\alpha}$). This number can be further reduced by the symmetries of the problem. In the XY model the global phase flip symmetry (global π rotation about the z axis) in the paramagnetic phase ($\lambda\leq1$) implies $[\sigma_i^z\sigma_j^z,\rho_{i,j}]=0$, which imposes that $\langle\sigma_i^{x(y)}\rangle=\langle\sigma_i^x\sigma_j^z\rangle=\langle\sigma_i^y\sigma_j^z\rangle=0$, leaving only five independent correlation functions: $\langle\sigma_i^z\rangle$, $\langle\sigma_i^\alpha\sigma_j^\alpha\rangle$, $\alpha=x,y,z$, and $\langle\sigma_i^x\sigma_j^y\rangle$. In the ferromagnetic phase ($\lambda>1$) this no longer holds since the Hamiltonian symmetry is not preserved by the ground state and we have to explicitly evaluate the nine one- and two-point correlation functions. $\langle\sigma_i^z\rangle$, $\langle\sigma_i^\alpha\sigma_j^\alpha\rangle$, $\alpha=x,y,z$, and $\langle\sigma_i^{x(y)}\rangle$ were obtained in Refs. [38,39]. We are left then with three off-diagonal two-point correlation functions to calculate $\langle\sigma_i^x\sigma_j^y\rangle$, $\langle\sigma_i^x\sigma_j^z\rangle$, and $\langle\sigma_i^y\sigma_j^z\rangle$. Finally, due to the translational symmetry of the model, $\rho_{i,j}$ depends only on the distance $n=|i-j|$ between the spins, $p_{i,j}^{\alpha,\beta}=p_n^{\alpha,\beta}$ and $p_i^{\alpha,0}\equiv p_i^\alpha=p^\alpha$ is the same for all spins.

We could be tempted to say that $\rho_{i,j}$ is real since the matrix elements of Hamiltonian (3.1) are all real, and use this fact to eliminate p_n^{xy} and p_n^{yz} as both quantities appear in $\rho_{i,j}$ multiplied by the imaginary i. However, this argument can be misleading since this "symmetry" is not preserved in the ferromagnetic state in the thermodynamic limit. As a counterexample consider for instance the Ising Hamiltonian with the nearest-neighbor coupling in the y direction and a magnetic field in the z direction ($\gamma=-1$). In the ferromagnetic phase we would have a finite value for $\langle\sigma_i^y\rangle$, which then results in complex elements in $\rho_{i,j}$. Fortunately, exact expressions for two of the three remaining off-diagonal correlation functions have been obtained by Johnson and McCoy [40]. In fact, they have calculated the full time-dependent correlation functions $\langle\sigma_i^y(0)\sigma_i^z(t)\rangle$ and $\langle\sigma_i^x(0)\sigma_i^z(t)\rangle$. In particular, they have shown that at any time t, $\langle\sigma_i^y(0)\sigma_i^z(t)\rangle=0$ for all values of γ and h, which leads to $p_n^{yz}=0$. For $\langle\sigma_i^x(0)\sigma_i^y(t)\rangle$, they have shown that the leading term for large n in both phases is linear in t, suggesting that p_n^{xy} ($t=0$) might be exactly zero. Numerical calculations of p_n^{xy} for small chains have confirmed that it does indeed vanish in both phases [49]. Collecting all the previous results the reduced two-spin density matrix $\rho_{i,j}$ can be written as

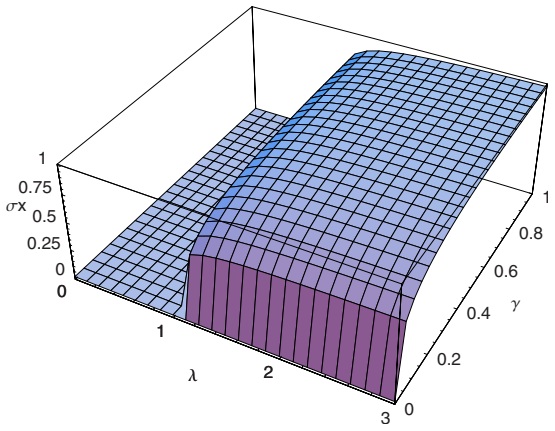

FIG. 1. (Color online) Magnetization along the x axis for the XY model, with anisotropy. The first transition, 1CP, is apparent from the discontinuity at $\lambda=1$, for any anisotropy γ.

$$\frac{1}{4}\begin{pmatrix}1+2p^z+p_{ij}^{zz} & p^x+p_{ij}^{xz} & p^x+p_{ij}^{xz} & p_{ij}^{xx}-p_{ij}^{yy}\\ p^x+p_{ij}^{xz} & 1-p_{ij}^{zz} & p_{ij}^{xx}+p_{ij}^{yy} & p^x-p_{ij}^{xz}\\ p^x+p_{ij}^{xz} & p_{ij}^{xx}+p_{ij}^{yy} & 1-p_{ij}^{zz} & p^x-p_{ij}^{xz}\\ p_{ij}^{xx}-p_{ij}^{yy} & p^x-p_{ij}^{xz} & p^x-p_{ij}^{xz} & 1-2p^z+p_{ij}^{zz}\end{pmatrix}. \tag{3.4}$$

The last off-diagonal correlation function p_n^{xz} was obtained in terms of cumbersome complex integrals in Ref. [40] rendering its explicit computation very tedious. However, we were able to obtain bounds for it from the physical restriction that all eigenvalues of $\rho_{i,j}$ must be positive. Considering one of its eigenvalues as a function of p_n^{xy} results in a second-degree polynomial with negative second derivative (we have checked this for many values of λ ranging from 0 to 3 and for γ ranging from 0.1 to 1). This allowed us to obtain tight lower and upper bounds for the value of p_n^{xz}. This completes our construction of the reduced density matrix of two spins, which is all we need for the calculation of entanglement. In Figs. 1–5 we plot the magnetization $\langle\sigma_i^\alpha\rangle$ along $\alpha=x,z$ and

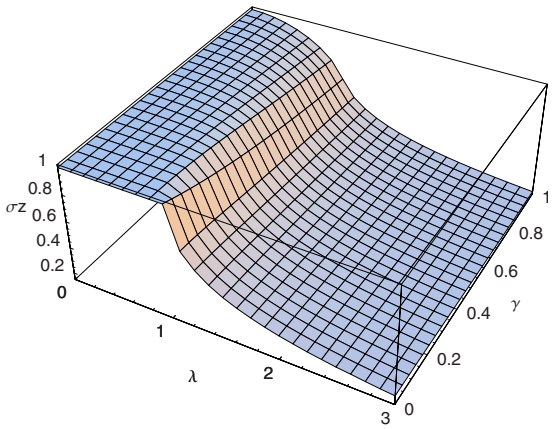

FIG. 2. (Color online) Magnetization along the z axis for the XY model.

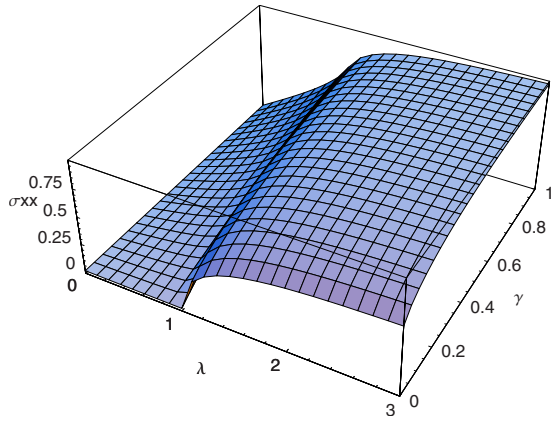

FIG. 3. (Color online) Nearest neighbor ($j=i\pm1$) diagonal correlation function $\langle\sigma_i^x\sigma_j^x\rangle$ for the XY model.

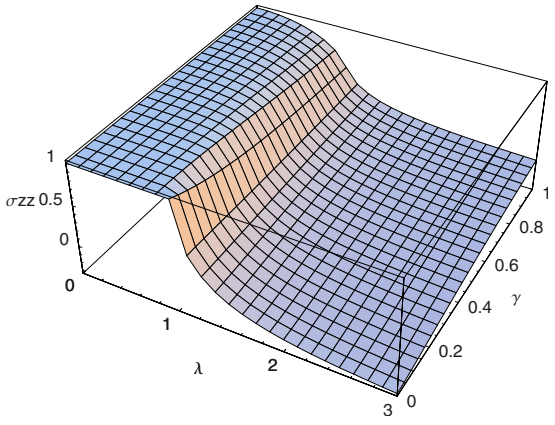

FIG. 5. (Color online) Nearest neighbor ($j=i\pm1$) diagonal correlation function $\langle\sigma_i^z\sigma_j^z\rangle$ for the XY model.

the diagonal correlation functions $\langle\sigma_i^\beta\sigma_j^\beta\rangle$, $\beta=x,y,z$ for nearest neighbors, $j=i\pm1$, for later discussion.

IV. BIPARTITE ENTANGLEMENT

The bipartite entanglement between a pair of two-level systems (qubits or $S=1/2$ spins) can be quantified using the concurrence C, since it is a monotonic function of the entanglement of formation [9], a well established measure. The concurrence can be obtained from the density matrix of the two spins and is given by $C=\max\{0,\epsilon_1-\epsilon_2-\epsilon_3-\epsilon_4\}$, where ϵ_i, $i=1,\ldots,4$, are the square roots of the eigenvalues, in decreasing order, of the matrix $R=\rho\tilde{\rho}$. Here $\tilde{\rho}=(\sigma^y\otimes\sigma^y)\rho^*(\sigma^y\otimes\sigma^y)$. Another pairwise measure of entanglement is the negativity which is based on the Peres-Horodecki separability test [50,51]. This test states that a separable state is always positive under partial transposition (PPT). This is also a sufficient condition for separability in the case of two-level systems. Thus, it is reasonable to quantify entanglement measuring "how much" the partially transposed density matrix is negative. A possible definition of negativity, which was proved to be an entanglement monotone [10], is given as $N(n)=\max\{0,-2\ \min(u_k)\}$, where u_k are the eigenvalues of the partial transpose of $\rho_{i,i+n}$ and the label n denotes the distance between the qubits. The main advantage of the negativity over the concurrence is that the former is easier to compute than the latter.

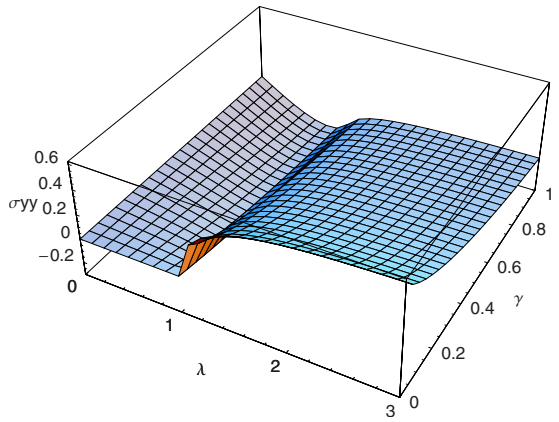

FIG. 4. (Color online) Nearest neighbor ($j=i\pm1$) diagonal correlation function $\langle\sigma_i^y\sigma_j^y\rangle$ for the XY model.

In the paramagnetic phase ($\lambda\leq1$), or for any value of λ in the symmetric ground state (i.e., without symmetry breaking), the concurrence and the negativity are simple expressions in terms of the correlation functions. Mathematically, this is a consequence of the fact that the fourth-degree equations resulting from the diagonalization of R factorize into two equations of the second degree [52]. The expression for the concurrence, valid for any system possessing the same symmetries as the symmetric ground state of the XY model is written as

$$C(n)=\max\{0,C'(n),C''(n)\}, \tag{4.1}$$

where

$$C'(n)=\frac{1}{2}(|p_n^{xx}-p_n^{yy}|+p_n^{zz}-1), \tag{4.2}$$

$$C''(n)=\frac{1}{2}[|p_n^{xx}+p_n^{yy}|-\sqrt{(1+p_n^{zz})^2-4(p^z)^2}]. \tag{4.3}$$

The negativity expression derived exclusively for the XY model reads

$$N(n)=\max\{0,-2\ \min[u_1(n),u_3(n)]\}, \tag{4.4}$$

where

$$u_1(n)=-\frac{1}{2}[1+p_n^{zz}-\sqrt{(p_n^{xx}+p_n^{yy})^2+4(p^z)^2}], \tag{4.5}$$

$$u_3(n)=-\frac{1}{2}(1-p_n^{xx}+p_n^{yy}-p_n^{zz}). \tag{4.6}$$

The expression for the concurrence could be written in this general form (independent of the particular values of the one and two-point correlation functions) because it is derived simply by imposing the positivity of $\rho_{i,j}$ and the fact that all eigenvalues of R are real numbers. We have also observed

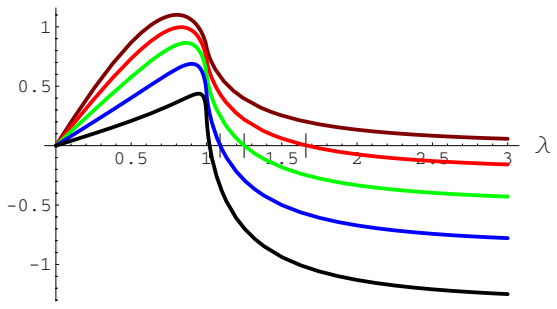

FIG. 6. (Color online) Plot of the left-hand side of Eq. (4.7) as a function of λ: when the function is positive the concurrence for the *XY* model does not change upon symmetry breaking. The anisotropies are $\gamma=1$, 0.8, 0.6, 0.4, and 0.2 (from top to bottom). We have also plotted a small vertical bar to represent the position of the 2CP $[\lambda_2(\gamma)=1/\sqrt{1-\gamma^2}]$.

that for $\gamma^2+1/\lambda^2>1$, i.e., $\lambda<\lambda_2(\gamma)$ it is always $C'(n)$ and $u_1(n)$ that are relevant for the concurrence and the negativity through Eqs. (4.1) and (4.4), respectively. On the other hand, for $\gamma^2+1/\lambda^2<1$, i.e., $\lambda>\lambda_2(\gamma)$, it is $C''(n)$ and $u_3(n)$ that appear in these two measures, respectively. The change from $\gamma^2+1/\lambda^2>1$ to $\gamma^2+1/\lambda^2<1$ occurs at the 2CP, i.e., at $\lambda=\lambda_2(\gamma)=1/\sqrt{1-\gamma^2}$.

In the ferromagnetic phase (for the broken-symmetry state) the calculation of the concurrence is not so simple since we have a fourth-degree equation which factorizes into a first-degree one and a complicated third-degree equation. Although the latter can be solved exactly, the expressions for its roots are not very illuminating, rendering a detailed general analysis unfeasible. Fortunately, it was demonstrated [52] that for the Ising model the concurrence does not change upon spontaneous symmetry breaking. This opened the possibility for the use of the simple expression of the paramagnetic phase in the ferromagnetic one. The analysis can be extended to the *XY* model since the reduced density matrices of the two models have a similar form. The condition for an identical expression for the concurrence in the paramagnetic and ferromagnetic phases is

$$\sqrt{(1+p_n^{zz})^2-4(p^z)^2}+p_n^{zz}-2p_n^{yy}-1>0. \qquad (4.7)$$

In Fig. 6 we show the left-hand side of Eq. (4.7) as a function of λ for the *XY* model. It can be seen that Eq. (4.7) always holds for the Ising model ($\gamma=1$, first curve from top to bottom) but is violated after the 2CP $[\lambda>\lambda_2(\gamma)=1/\sqrt{1-\gamma^2}]$ in the *XY* model ($\gamma\neq 1$). The critical value $\lambda_2(\gamma)$ has been indicated by the vertical lines for each γ in Fig. 6.

Using the above expressions and the correlation functions depicted in Figs. 1–5, including the bounds for p_n^{xz} obtained through the procedure explained in Sec. III, we now analyze the bipartite entanglement between any two spins of the *XY* chain. Notice that for the following discussion we have calculated numerically the concurrence, not relying in the simplified formula (4.1). First, we have evaluated the concurrence of nearest neighbors $[C(1)]$ for some values of the anisotropy γ. These results are shown in Fig. 7, where we plot the lower bounds for the concurrence. Moreover, in Fig. 8 we show both the lower and the upper bounds for the broken-symmetry state as well as the concurrence in the unphysical symmetric ground state. As is already known [6,7], $C(1)$ is not maximal at the 1CP. It is important to note that the bounds are very tight near the QPTs allowing us to correctly characterize the behavior of the concurrence at the CPs. Indeed, Fig. 8 shows that the concurrence changes more abruptly (a diverging derivative) at the 2CP than at the 1CP where the spontaneous symmetry breaking occurs ($\lambda=\lambda_1=1$). We can also see that after the 1CP the concurrence starts to decrease, vanishing at the 2CP. This fact had already been observed [24] and it can be shown that at this point the ground state is completely separable [24].

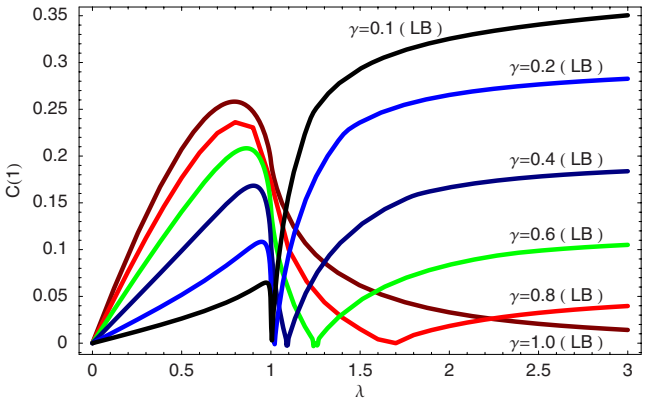

FIG. 7. (Color online) Lower bound of the concurrence for nearest neighbors obtained using the upper bound of p_1^{xz}. In the limit of small magnetic field (large λ) the entanglement decreases with increasing γ. Here $\gamma=1,0.8,0.6,0.4,0.2$, and 0.1 from top to bottom in the $\lambda\leq 1$ phase.

Remarkably, the discrepancy between the symmetric and the broken-symmetry cases, in contrast to what one might expect, only occurs after the 2CP ($\lambda>\lambda_2$), where the correlation functions tend to their limiting value in an oscillatory fashion [39]. Thus, the spontaneous symmetry breaking, which occurs already at the 1CP, has no influence on bipartite entanglement. Even after the 2CP the difference between

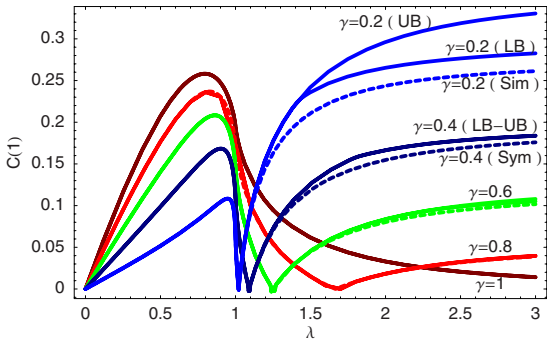

FIG. 8. (Color online) The lower and upper bounds for the nearest-neighbor concurrence (solid lines) and the concurrence in the symmetric state (dashed lines). Here $\gamma=1,0.8,0.6,0.4$, and 0.2 from top to bottom in the $\lambda\leq 1$ phase. Note that for most of the anisotropies we can barely see the difference between the lower and upper bounds.

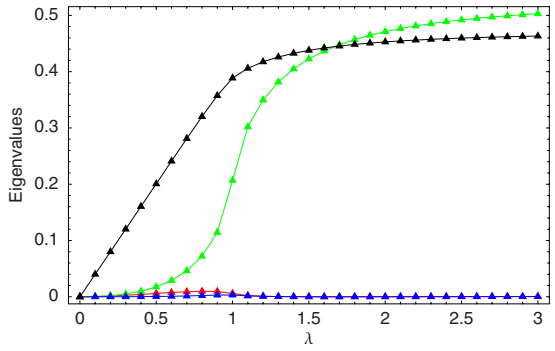

FIG. 9. (Color online) Plot of the square root of the eingenvalues of the matrix R (for $\gamma=0.8$), used to obtain the concurrence, for the symmetric case. We can observe a change in the greatest eigenvalue of R at the second critical point resulting in a change from $C'(n)$ to $C''(n)$ as the expression that contributes to the concurrence.

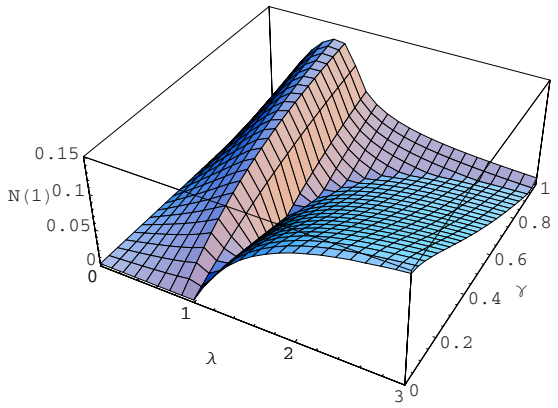

FIG. 11. (Color online) Nearest neighbor negativity in the symmetric ground state. We can see that at the critical point the entanglement decreases as we approach the XX model ($\gamma\rightarrow 0$).

the symmetric and the broken-symmetry states is small and becomes more pronounced only as $\gamma\rightarrow 0$, where the former has slightly less entanglement than the latter. Finally, the "origin" of the entanglement is different in the two states since in the symmetric case at the 2CP there is a change in the greatest eigenvalue of R, see Fig. 9 [this results in a change from $C'(n)$ to $C''(n)$ as the expression that contributes to the concurrence]. This has been interpreted [24] as a change in the kind of entanglement present in the ground state. However, this is not true when one correctly employs the broken-symmetry state since now it is the same eigenvalue of R that is maximal for all values of λ, see Fig. 10. We can also see that, as we approach the XX model ($\gamma\rightarrow 0$), the concurrence decreases in the $\lambda<1$ region, vanishing at the 1CP, and then increases in the ferromagnetic phase ($\lambda>1$).

Similar conclusions can be derived for the negativity since the curves for the negativity as a function of λ and γ are very close to the ones already shown for the concurrence. Here we only plot the negativity for nearest neighbors $N(1)$ in the symmetric state in Fig. 11. We should note that, as for the concurrence, the negativity of the symmetric ground state is close to the negativity of the broken-symmetry state in the ferromagnetic phase.

We have also obtained the concurrence between next-nearest neighbors $C(2)$ in the broken-symmetry state. In Fig. 12 we show its lower bound for some values of γ. We can see that in contrast to $C(1)$, $C(2)$ at first increases in the paramagnetic phase as we leave the Ising model in the direction of the XX model. As a function of λ, $C(2)$ reaches its maximal value just before $\lambda=1$ (the 1CP), which increases as $\gamma\rightarrow 0$. For small magnetic field (large λ) we see the same behavior as for $C(1)$: the entanglement increases as we approach the XX model ($\gamma\rightarrow 0$). The difference in the entanglement of the symmetric and the broken-symmetry states, however, is more pronounced now. In contrast to the broken-symmetry state, the entanglement in the symmetric state vanishes for λ larger than a certain value. This is illustrated in Fig. 13 where we show the lower and upper bounds for the concurrence in the broken-symmetry state compared to the concurrence in the symmetric state for $\gamma=0.2$. We should note that for all values of $\gamma>0.2$, the bounds are tighter in comparison.

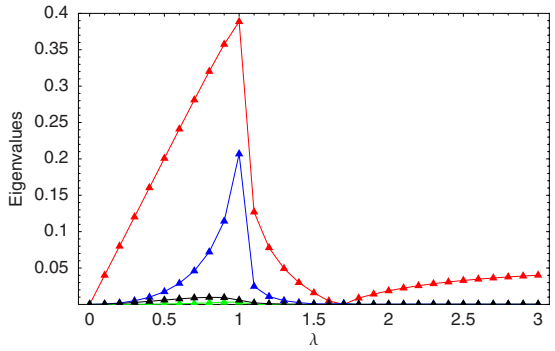

FIG. 10. (Color online) Plot of the square root of the eingenvalues of the matrix R (for $\gamma=0.8$), used to obtain the concurrence, for the broken-symmetry case. We can observe that for the broken-symmetry case there is no crossing of eigenvalues of R at the second critical point. Actually, all eigenvalues vanish at the 2CP. This plot was obtained using the upper bound for p^{xz} but there is no visible difference if we use the lower bound.

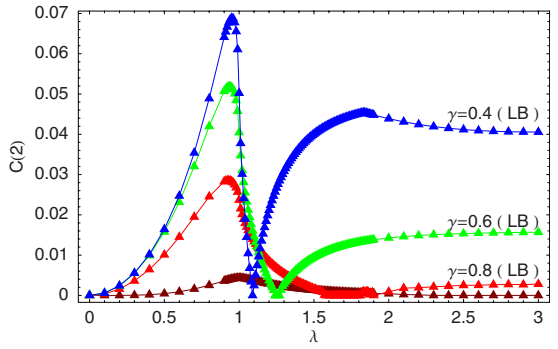

FIG. 12. (Color online) Lower bound for the concurrence for next-nearest neighbors using the upper bounds of the off-diagonal correlation function p_2^{xz}. Here $\gamma=1,0.8,0.6$, and 0.4 from bottom to top in the $\lambda\leq 1$ phase. The broken-symmetry state was used in the ferromagnetic phase ($\lambda>1$).

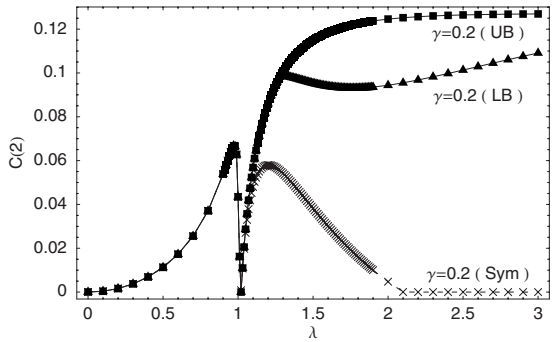

FIG. 13. Concurrence for next-nearest neighbors in the broken-symmetry state at $\gamma=0.2$, obtained using the upper (triangles) and lower (squares) bounds of the off-diagonal correlation function p_2^{xz}. For comparison, we also plot the concurrence in the symmetric state (crosses).

The negativity for next-nearest neighbors has a similar behavior but with smaller values in the region of small fields (large λ). This can be better viewed in Fig. 14 where we plot $N(2)$ in the symmetric state. Note that in the symmetric state the negativity (and also the concurrence) vanishes for sufficiently small values of the field.

We have also calculated the concurrence and the negativity for spins three and four lattice sites apart, which show behaviors similar to $C(2)$ and $N(2)$. The only difference is that the entanglement is much smaller, decreasing as we increase the distance between the spins. It should be noted that the concurrence and negativity values for next-nearest neighbors are significantly smaller than the ones for nearest neighbors, which means that bipartite entanglement is more concentrated on nearest-neighbor sites.

One last fact about bipartite entanglement which we would like to mention is related to the origin of the nonanalyticities of the concurrence and of the ground-state energy per site $\mathcal{E}$. It terms of the two spin reduced density matrix elements $(\rho_{i,j})_{\alpha\beta}=(\rho)_{\alpha\beta}$ we have

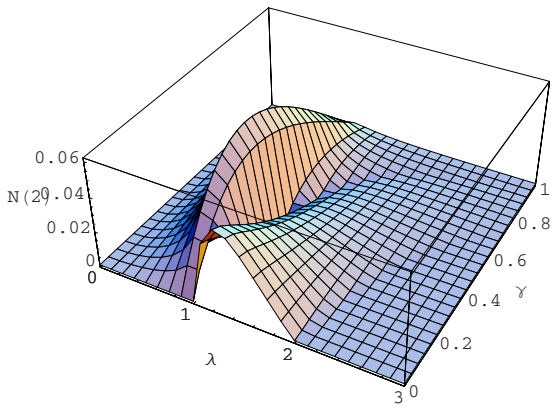

FIG. 14. (Color online) Negativity for next-nearest neighbors in the symmetric ground state. We can see that at the first critical point ($\lambda=1$) the entanglement first increases as we leave the XX model ($\gamma=0$) and then starts to decrease for sufficiently large γ.

$$\partial_\lambda^2 \mathcal{E} = -\frac{2}{\lambda}\partial_\lambda[(\rho)_{22}+(\rho)_{44}] \tag{4.8}$$

and

$$C(1) = 2[(\rho)_{41}-(\rho)_{22}], \tag{4.9}$$

where $C(1)$ is the concurrence for the symmetric case and ∂_λ^2 stands for the second order derivative with respect to the tuning parameter λ. As argued in Ref. [8] both $\partial_\lambda^2\mathcal{E}$ and $\partial_\lambda C(1)$ exhibit critical behavior through their dependence upon $\partial_\lambda(\rho)_{22}$, since $(\rho)_{41}$ is well behaved. Looking at the correlation functions we observe that the divergence of $\partial_\lambda(\rho)_{22}$ comes from the correlation in the z direction as $(\rho)_{22}=1-p^{zz}$. However $(\rho)_{44}$ also has a dependence on p^{zz} which cancels the one in $(\rho)_{22}$, and we end up with

$$\partial_\lambda^2 \mathcal{E} = -\frac{1}{\lambda}\partial_\lambda p^z. \tag{4.10}$$

Therefore, in terms of the correlation functions, the critical behavior of $\partial_\lambda^2\mathcal{E}$ is originated on p^z while the divergence of $\partial_\lambda C(1)$ is given by p^{zz}, since $(\rho)_{41}=p^{xx}-p^{yy}$ does not cancel the divergence of p^{zz}.

In sum, based on these measures of entanglement we can say that there is more bipartite entanglement around the 1CP when we approach the Ising model. When we approach the XX model the entanglement is more pronounced in the ferromagnetic phase. We expect this behavior to continue to hold for $C(n)$ and $N(n)$ when $n>4$. It has already been pointed out that the range in which the concurrence has a finite value increases as $1/\gamma$ [7], being infinite for the XX model. Finally, we would like to stress that the concurrence does not change upon symmetry breaking in the Ising model. This fact shows that it suffers no influence during the symmetry-breaking process, although bipartite entanglement is able to mark the phase transition through a diverging derivative of the concurrence.

In the XY model, on the other hand, the concurrence is different for symmetric and broken-symmetry states. However, this difference only appears at the second critical point, not as a result of the symmetry breaking that occurs at the first critical point. Thus, we have shown that for both the Ising and the XY model, the symmetry-breaking phase transition does not affect the bipartite entanglement. In fact, as three of us have already argued [42], the fact that the concurrence does not depend on the magnetization in the x direction p^x is a possible explanation for the fact that it is not maximal at the critical point.

V. MULTIPARTITE ENTANGLEMENT

After studying the entanglement between two spins in the chain we now focus our attention on the multipartite entanglement (ME) in the XY model as given by $G(1)$ [43] and $G(2,n)$ [41,42,44]. For a spin-1/2 chain these are given by

$$G(1) = \frac{d}{d-1}\left[1-\frac{1}{N}\sum_{j=1}^{N}\mathrm{Tr}(\rho_j^2)\right] \tag{5.1}$$

and

$$G(2,n) = \frac{d}{d-1}\left[1 - \frac{1}{N-n}\sum_{j=1}^{N-n} \mathrm{Tr}(\rho_{j,j+n}^2)\right], \qquad (5.2)$$

where d is the dimension of the Hilbert space of the reduced density matrices ρ_j or $\rho_{j,j+n}$, i.e., $d=2$ for $G(1)$ and $d=4$ for $G(2,n)$. For systems with translational invariance such as the XY model, these measures simply reduce to the linear entropy of one- and two-spin n sites apart, respectively.

One advantage of the measures (5.1) and (5.2) is that they are simple to evaluate since we just need the reduced one- and two-spin density matrices that were already obtained previously. This kind of measure has received the name of local entanglement measure or estimator since they depend on the reduced density operator of two spins, which is a local quantity. Moreover, inspired by accumulated experience of many-body physics, we believe that a great deal can be learned from the knowledge of two-point correlation functions only. $G(2,n)$ inherits the full nonanalytical behavior of the elements of the reduced density matrix of two spins and it is possible to make a general link between divergences in the derivatives of the energy, which signal QPTs, and $G(2,n)$ or its derivatives [44]. In other words, $G(2,n)$ and/or its derivatives are able to signal QPTs as do bipartite entanglement measures, with the exceptions of the cases where the nonanalyticities accidentally cancel out. In Ref. [44] it was shown that $G(1)$ and $G(2,n)$ are maximal at the 1CP and zero at the 2CP, thus possessing the ability to map out the complete phase diagram of the XY model. Here we intend to analyze those results in vision of the differences between the symmetric and broken-symmetry cases and states.

For the XY model Eqs. (5.1) and (5.2) above can be rewritten in terms of the one and two-point correlation functions, depicted in Figs. 1–5, as

$$G(1) = 1 - \langle\sigma_j^x\rangle^2 - \langle\sigma_j^z\rangle^2 \qquad (5.3)$$

and

$$G(2,n) = 1 - \frac{1}{3}(2\langle\sigma_j^x\rangle^2 + 2\langle\sigma_j^z\rangle^2 + 2\langle\sigma_j^x\sigma_{j+n}^z\rangle^2 + \langle\sigma_j^x\sigma_{j+n}^x\rangle^2 + \langle\sigma_j^y\sigma_{j+n}^y\rangle^2 + \langle\sigma_j^z\sigma_{j+n}^z\rangle^2). \qquad (5.4)$$

As we mentioned before, Eqs. (5.3) and (5.4) have already been shown to be maximal at the 1CP of the Ising [41] and XY [44] models. We have argued that this behavior is due to the emergence of a finite value of the magnetization with the spontaneous symmetry breaking for $\lambda > 1$, since this is the correlation function in the expressions for $G(1)$ and $G(2,n)$ exhibiting the most abrupt change, despite being continuous at the 1CP. This will be made clearer as we investigate the behavior in the symmetric case. We also note that at the 1CP $G(2,n)$ always increases as a function of n which is a strong indication of genuine ME. The von Neumann entropy (entropy of entanglement) of one spin has already been shown to be maximal at the 1CP [6].

We first show $G(1)$ for the XY model as a function of λ and γ for the broken-symmetry case (see Fig. 15). We can see that for all values of the anisotropy $G(1)$ is maximal at the 1CP and decreases as one approaches the XX model. We have also checked that $G(1)$ is zero at the 2CP $\lambda=\lambda_2(\gamma)=1/\sqrt{1-\gamma^2}$ as expected, since at this point the state is completely separable [24].

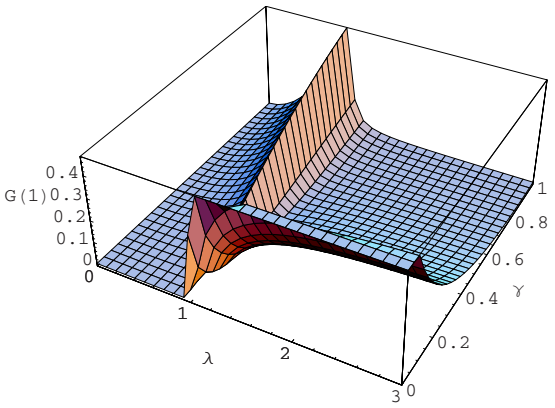

FIG. 15. (Color online) $G(1)$ for the XY model in the broken-symmetry case.

The upper bound for $G(2,1)$ for the broken-symmetry case is shown in Fig. 16. We note that it behaves similarly to $G(1)$. To check the quality of the bounds we also plot the lower and upper bounds for $G(2,1)$ in the broken-symmetry case for three values of anisotropy in Fig. 17. The same behavior was also found for $G(2,2)$ and $G(2,7)$ [44]. In fact, the value of $G(2,n)$ for a fixed λ always increases as a function of n, which is in contrast to bipartite entanglement, and also in contrast to the correlation functions, which decrease as n increases. Therefore, $G(2,n)$ must increase [see Eq. (5.4)], either as a power law at the critical point or exponentially away from it. As mentioned before, this feature allows the definition of an entanglement length (see Ref. [44] for more details) and indicates that at the CP the entanglement is more distributed in the chain than anywhere else.

Since both $G(1)$ and $G(2,n)$ essentially show the same behavior, from Eq. (5.3) we conclude that the magnetizations $\langle\sigma_j^x\rangle$ and $\langle\sigma_j^z\rangle$ are the minimal quantities from which the multipartite entanglement over the chain can be inferred. Now we observe that near the XX model ($\gamma\to 0$) the ferromagnetic phase shows more entanglement than the CP, a feature ob-

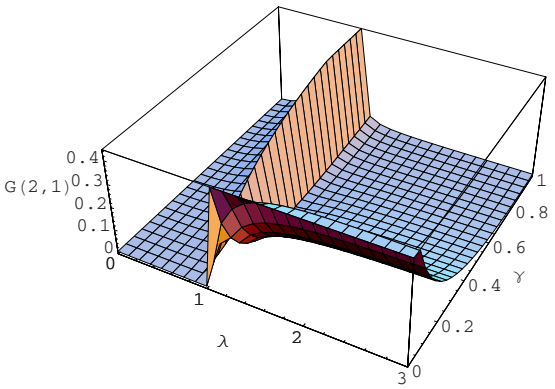

FIG. 16. (Color online) $G(2,1)$ for the XY model in the broken-symmetry case.

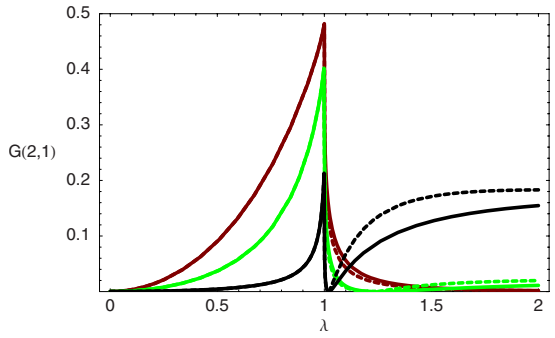

FIG. 17. (Color online) Lower (solid lines) and upper (dashed lines) bounds for $G(2,1)$ of the XY model in the broken-symmetry case for three values of the anisotropy: $\gamma=1,0.6,0.2$ (from top to bottom in the $\lambda<1$ region).

served for bipartite entanglement between two spins as well, as given by the concurrence and negativity (see Figs. 7 and 11). This behavior should be contrasted with Figs. 1–5 for the magnetization and diagonal correlations. Notice that those one and two-point correlations (apart from $\langle\sigma_i^y\sigma_j^y\rangle$) are invariably smaller closer to the XX model than closer to the Ising model, in particular $\langle\sigma_j^x\rangle$ and $\langle\sigma_j^z\rangle$, showing the well know fact that, deep in the ferromagnetic phase the magnetization is destroyed by quantum fluctuations as ones goes from the Ising Hamiltonian to the XX limit. Thus it is reassuring to see that the proposed indicators of "quantum character," both bipartite and multipartite entanglement measures, do indeed increase as we approach the XX model from the Ising one. This feature highlights the differences between classical and quantum correlations (entanglement) in the XY model. Thus, although the correlation functions involve both classical and quantum correlations, only a proper combination of them can reveal their entanglement content.

We now compare the symmetric and broken-symmetry states. In Fig. 18 we have plotted $G(1)$ and in Fig. 19 $G(2,1)$, both for two values of the anisotropy $\gamma=1$ and $\gamma=0.4$. It can be seen that in both cases the symmetric state (dashed line) does not show a maximum at the 1CP. Instead, it is an increasing monotonic function of λ. The crucial element here is that the magnetization in the x direction $\langle\sigma^x\rangle$

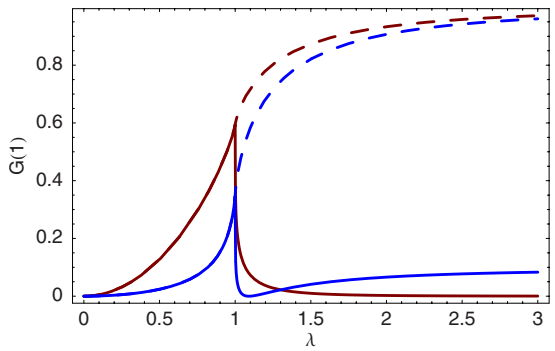

FIG. 18. (Color online) Comparison of $G(1)$ in the symmetric (dashed lines) and broken-symmetry (solid lines) states for the XY model and for two values of anisotropy: $\gamma=1$ (brown) and 0.4 (blue).

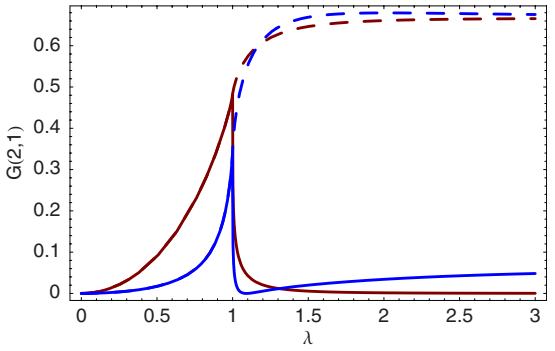

FIG. 19. (Color online) Comparison of $G(2,1)$ in the symmetric (dashed lines) and broken-symmetry (solid lines) states for the XY model and for two values of anisotropy: $\gamma=1$ (brown) and 0.4 (blue).

and $\langle\sigma_i^x\sigma_j^z\rangle$ vanish in the region $\lambda>1$ in the symmetric case, and the former is responsible for the difference in behavior between $G(1)$ and $G(2,1)$. To check this, we have made $\langle\sigma^x\rangle$ zero by hand in the expression for $G(2,1)$ in the broken-symmetry case and verified that the result is very similar to the symmetric case. This indicates that the magnetization is the primary reason why $G(1)$ and $G(2,1)$ are maximal at the 1CP and the results for the symmetric and broken-symmetry cases are different. The reader should remember that in the case of bipartite entanglement, given by the concurrence or the negativity, spontaneous symmetry breaking had no effect, only appearing to contribute in a different manner after the 2CP. Furthermore, we observe that both $G(1)$ and $G(2,n)$ signal the two critical points in the broken-symmetry state, while the same is not true in the symmetric state. The complete phase diagram could thus be drawn only by considering the nonanalyticities of either of these two measures. Thus symmetry-breaking has more effect over multipartite entanglement. Again, the presence of the magnetization $\langle\sigma^x\rangle$ (which is highly sensitive to symmetry breaking) in both $G(1)$ and $G(2,n)$ and its absence in the concurrence and negativity is responsible for the different behavior when one uses a broken symmetry ground state or not.

VI. CONCLUSIONS

We have extensively studied the entanglement properties of the one-dimensional XY model in a transverse magnetic field. We have in all cases assumed the chain to be at $T=0$ and worked in the thermodynamic limit of an infinite chain. One of our goals was to characterize both the pairwise and multipartite entanglement of the ground state of the XY model. In order to do a complete analysis we were forced to consider two distinct ground states. The first one, which always preserves all the symmetries of the Hamiltonian, was called the symmetric ground state. This state, however, is unphysical for $\lambda=J/h>1$ since in a realistic situation the global phase flip (global π rotation around the z axis) is always spontaneously broken. Therefore, we also considered a second state, namely, the broken-symmetry ground state, where this symmetry no longer holds.

For the broken-symmetry state we were able to show that, in contrast to pairwise entanglement, multipartite entanglement is maximal at the first critical point (where the *XY* model exhibits a diverging correlation length). This property is not observed in the symmetric state, in which case the multipartite entanglement increases monotonically as we decrease the external magnetic field. Furthermore, we have also shown that the concurrence does not change in the vicinity of the symmetry-breaking critical point whether we employ the symmetric or the broken-symmetry state. On the other hand, we have explicitly shown that the multipartite entanglement depends strongly on the symmetry of the ground state. This result suggests that, as is the case for the *XY* model, the behavior of the multipartite entanglement may be intimately connected with the spontaneous symmetry breaking mechanism. We should also remark that only after the second critical point is the concurrence dependent on which state we use, and this is probably because the symmetry breaking has a more pronounced effect in the oscillatory behavior the correlations show after this point.

We have arrived at another interesting result by noticing two important facts. First, for spins three or more sites apart there exists no pairwise entanglement whatsoever [6,7]. Second, we have shown that multipartite entanglement is never zero at the first critical point (being maximal for the broken-symmetry state). Combining these two facts we are led to conclude that the long-range correlations at this critical point are a consequence of the existence of multipartite entanglement and not pairwise entanglement. Moreover both multipartite and bipartite entanglement tend to be larger than at the 1CP in the ferromagnetic phase as one approaches the *XX* model ($\gamma \to 0$), increasing monotonically after the 2CP. This feature contrasts with the one- and two-point correlations that tend to decrease as $\gamma \to 0$, showing that the enhanced quantum correlations (entanglement) in this region can only be appreciated through a proper combination of the correlation functions. Since the *XX* model belongs to a different universality class, nothing can be said about entanglement at $\gamma=0$ from our study. It would be certainly interesting to investigate how entanglement develops in the distinct phases of the *XX* model.

Finally, our results have shown that the entanglement contents of the two possible ground states, i.e., the symmetric and the broken-symmetry state, are different. Therefore, it is of utmost importance to clearly and explicitly verify which state one is using in any entanglement analysis made for the *XY* and related models in order to avoid any possible confusion.

Note added. Recently, we became aware of a work where the effects of symmetry breaking on the concurrence are also addressed [53], and a detailed study of the concurrence and the entanglement between one site and the rest of the chain (one tangle) [54].

ACKNOWLEDGMENTS

We acknowledge a couple of email exchanges between A. Osterloh and one of us (T.R.O.), which helped us to understand some statements made in Ref. [53]. We thank Amir O. Caldeira for clarifying discussions about ME and QPT. We acknowledge support from FAPESP through Grants Nos. 2005/00155-8 (T.R.O.), 2005/01441-4 (G.R.), and 04/14605-2 (M.C.O.), and from CNPq through grants Nos. 305971/2004-2 (E.M.), 303918/2005-5 (M.C.O.). This work was also partially supported by the Millennium Institute for Quantum Information.

[1] P. W. Anderson, *Basic Notions of Condensed Matter Physics* (Benjamin/Cummings, Menlo Park, 1984).
[2] S. Sachdev, *Quantum Phase Transitions* (Cambridge University Press, Cambridge, 2001).
[3] M. A. Nielsen and I. L. Chuang, *Quantum Computation and Quantum Information* (Cambridge University Press, Cambridge, 2000).
[4] P. Zanardi, Phys. Rev. A **65**, 042101 (2002); P. Zanardi and X. Wang, J. Phys. A **35**, 7947 (2002).
[5] T. J. Osborne and M. A. Nielsen, Quantum Inf. Process. **1**, 45 (2002).
[6] T. J. Osborne and M. A. Nielsen, Phys. Rev. A **66**, 032110 (2002).
[7] A. Osterloh, L. Amico, G. Falci, and R. Fazio, Nature (London) **416**, 608 (2002).
[8] L.-A. Wu, M. S. Sarandy, and D. A. Lidar, Phys. Rev. Lett. **93**, 250404 (2004).
[9] W. K. Wootters, Phys. Rev. Lett. **80**, 2245 (1998).
[10] G. Vidal and R. F. Werner, Phys. Rev. A **65**, 032314 (2002).
[11] L. Campos Venuti, C. Degli Esposti Boschi, M. Roncaglia, and A. Scaramucci, Phys. Rev. A **73**, 010303(R) (2006).
[12] L.-A. Wu, M. S. Sarandy, D. A. Lidar, and L. J. Sham, Phys. Rev. A **74**, 052335 (2006).
[13] M.-F. Yang, Phys. Rev. A **71**, 030302(R) (2005).
[14] J. Vidal, Phys. Rev. A **73**, 062318 (2006).
[15] S.-J. Gu, G.-S. Tian, and H.-Q. Lin, N. J. Phys. **8**, 61 (2006).
[16] D. Larsson and H. Johannesson, Phys. Rev. A **73**, 042320 (2006).
[17] X. Wang, Phys. Rev. A **64**, 012313 (2001).
[18] J. I. Latorre, E. Rico, and G. Vidal, Quantum Inf. Comput. **4**, 48 (2004).
[19] G. Vidal, J. I. Latorre, E. Rico, and A. Kitaev, Phys. Rev. Lett. **90**, 227902 (2003).
[20] C. Holzhey, F. Larsen, and F. Wilczek, Nucl. Phys. B **424**, 443 (1994).
[21] P. Calabrese and J. Cardy, J. Stat. Mech.: Theory Exp. (2004), P06002 .
[22] A. R. Its, B.-Q. Jin, and V. E. Korepin, J. Phys. A **38**, 2975 (2005); e-print arXiv:quant-ph/0606178v3; F. Franchini, A. R. Its, B.-Q. Jin, and V. E. Korepin, e-print arXiv:quant-ph/0606240v1.
[23] T.-C. Wei, D. Das, S. Mukhopadyay, S. Vishveshwara, and P. M. Goldbart, Phys. Rev. A **71**, 060305(R) (2005).
[24] L. Amico, F. Baroni, A. Fubini, D. Patanè, V. Tognetti, and P.

Verrucchi, Phys. Rev. A **74**, 022322 (2006).
[25] V. Coffman, J. Kundu, and W. K. Wootters, Phys. Rev. A **61**, 052306 (2000).
[26] P. Stelmachovic and V. Buzek, Phys. Rev. A **70**, 032313 (2004).
[27] F. Verstraete, M. Popp, and J. I. Cirac, Phys. Rev. Lett. **92**, 027901 (2004); M. Popp, F. Verstraete, M. A. Martín-Delgado, and J. I. Cirac, Phys. Rev. A **71**, 042306 (2005).
[28] F. Verstraete, M. A. Martin-Delgado, and J. I. Cirac, Phys. Rev. Lett. **92**, 087201 (2004).
[29] G. Gour and R. W. Spekkens, Phys. Rev. A **73**, 062331 (2006).
[30] P. Zanardi and N. Paunković, Phys. Rev. E **74**, 031123 (2006); P. Zanardi, P. Giorda, and M. Cozzini, e-print arXiv:quant-ph/0701061v1.
[31] L. Amico, A. Osterloh, F. Plastina, R. Fazio, and G. M. Palma, Phys. Rev. A **69**, 022304 (2004).
[32] T. Roscilde, P. Verrucchi, A. Fubini, S. Haas, and V. Tognetti, Phys. Rev. Lett. **93**, 167203 (2004); A. Anfossi, P. Giorda, A. Montorsi, and F. Traversa, *ibid.* **95**, 207206 (2005).
[33] H. Fan, V. Korepin, and V. Roychowdhury, Phys. Rev. Lett. **93**, 227203 (2004).
[34] Y. Chen, P. Zanardi, Z. D. Wang, and F. C. Zhang, New J. Phys. **8**, 97 (2006).
[35] Y. Chen, Z. D. Wang, and F. C. Zhang, Phys. Rev. B **73**, 224414 (2006).
[36] J. I. Latorre, C. A. Lütken, E. Rico, and G. Vidal, Phys. Rev. A **71**, 034301 (2005).
[37] P. Pfeuty, Ann. Phys. (N.Y.) **57**, 79 (1970).
[38] E. Barouch, B. M. McCoy, and M. Dresden, Phys. Rev. A **2**, 1075 (1970).
[39] E. Barouch and B. M. McCoy, Phys. Rev. A **3**, 786 (1971).
[40] J. D. Johnson and B. M. McCoy, Phys. Rev. A **4**, 2314 (1971).
[41] T. R. de Oliveira, G. Rigolin, and M. C. de Oliveira, Phys. Rev. A **73**, 010305(R) (2006).
[42] G. Rigolin, T. R. de Oliveira, and M. C. de Oliveira, Phys. Rev. A **74**, 022314 (2006).
[43] D. A. Meyer and N. R. Wallach, J. Math. Phys. **43**, 4273 (2002).
[44] T. R. de Oliveira, G. Rigolin, M. C. de Oliveira, and E. Miranda, Phys. Rev. Lett. **97**, 170401 (2006).
[45] The literature on entanglement in quantum phase transitions is already too extensive to be fully listed in this Introduction. We simply outline key papers related to the main subjects discussed in our developments. For a recent review on entanglement in many-body system see L. Amico, R. Fazio, A. Osterloh, and V. Vedral, e-print arXiv:quant-ph/0703044v1.
[46] G. K. Brennen, Quantum Inf. Comput. **3**, 619 (2003).
[47] A. J. Scott, Phys. Rev. A **69**, 052330 (2004).
[48] For perhaps the earliest discussion of why and how this comes about, see P. W. Anderson, Phys. Rev. **86**, 694 (1952).
[49] P. A. Vieira (private communication).
[50] A. Peres, Phys. Rev. Lett. **77**, 1413 (1996).
[51] M. Horodecki, P. Horodecki, and R. Horodecki, Phys. Lett. A **223**, 1 (1996).
[52] O. F. Syljuåsen, Phys. Rev. A **68**, 060301(R) (2003).
[53] A. Osterloh, G. Palacios, and S. Montangero, Phys. Rev. Lett. **97**, 257201 (2006).
[54] F. Baroni, A. Fubini, V. Tognetti, and P. Verrucchi, J. Phys. A **40**, 9845 (2007).